Smooth inversion for ground surface temperature histories: estimating the optimum regularization parameter by generalized cross-validation

V. Rath and D. Mottaghy

Applied Geophysics, RWTH Aachen University, Lochnerstr., 4-20, D-52056 *Aachen, Germany. E-mail: v.rath@geophysik.rwth-aachen.de*

Accepted 2007 August 19. Received 2007 August 19; in original form 2006 July 10

SUMMARY

The inversion of recent borehole temperatures has proved to be a successful tool to determine ancient ground surface temperature histories. To take into account heterogeneity of thermal properties and their non-linear dependence on temperature itself, a versatile 1-D inversion technique based on a finite-difference approach has been developed. Regularization of the generally ill-posed problem is obtained by an appropriate version of Tikhonov regularization of variable order. In this approach, a regularization parameter has to be determined, representing a trade-off between data fit and model smoothness. We propose to select this parameter by generalized cross-validation. The resulting technique is employed in case studies from the Kola ultradeep drilling site, and another borehole from northeastern Poland. Comparing the results from both sites corroborates the hypothesis that subglacial ground surface temperatures as met in Kola often are much higher than the ones in areas exposed to atmospheric conditions (Poland).

Key words: GCV, geothermics, inverse problem, palaeoclimate, regularization.

1 INTRODUCTION

In recent years, geothermal logs have been used to reconstruct ground surface temperature histories (GSTH) (Nielsen & Beck 1989; Dahl-Jensen *et al.* 1998; Pollack *et al.* 1998; Huang *et al.* 2000; Šafanda & Rajver 2001; Kukkonen & Joeleht 2003). Problems are that the temporal resolution of the reconstruction is low and the coupling of surface air temperature to ground temperature is still not well understood. Nevertheless such reconstructions represent the most direct record of past temperatures and are potentially valuable in analysing past climate conditions. Reconstructions have been carried out on various timescales from a few hundred to 100 000 yr by several authors. While the short-time reconstructions serve to investigate natural and anthropogenic climate change, the longer reconstructions aim to understand temperature variations back to the last Glacial and its transition to our current climate.

In the field of geothermal and hydrogeological research, the correction for palaeoclimatic effects is important to obtain reliable estimates of temperature gradients and heat flow. Temperature anomalies due to the slow motion of groundwater driven by topographic potential differences may easily reach a few Kelvin, which is the same order of magnitude as the climatic disturbance of subsurface temperatures related to the end of the last ice age (Kohl 1998). When trying to separate advective from conductive heat transport in a quantitative way, correction for palaeoclimate is a prerequisite. In practice, the ubiquitous presence of advective heat transport is one of the most prominent problems for estimating past surface temperatures.

We have not included these effects here for several reasons discussed below. For the inversion we employ a 1-D forward model. Although it is easy to implement a uniform vertical fluid flow into the finite-difference model applied for the forward modelling, it is of limited value. Such simple flow conditions are not often met in nature, with the notable exception of near-surface regimes ($>$100 m), as pointed out by Taniguchi (1993). A simple remedy like the inclusion of non-uniform flow fields into a 1-D model, increases the number of degrees of freedom for an inversion: constraints are difficult to derive. A more general treatment should include horizontal or subhorizontal fluid flow which is ubiquitous in sedimentary basins, and will redistribute the heat laterally (Vasseur *et al.* 1993; Zschocke *et al.* 2005; Ferguson *et al.* 2006). This regime can only be fully understood using 2- or 3-D model geometries, and can not be assumed to be constant with time. Full 3-D inversions, however, remain a task for the future.

Therefore, care has to be taken that no or only small amounts of advective heat transport are present near the borehole when inverting for GSTH. This hypothesis is often plausible, though it has to stand falsification in every case considered. Fortunately, the joint inversion of different boreholes often gives an excellent opportunity to reduce or even eliminate fluid flow effects, due to destructive interference of the groundwater flow signal in different boreholes. It has to be assumed however, that the spatial correlation structures of petrophysical properties, and the timescales of flow conditions are

sufficiently distinct from GST changes. Mean surface temperatures have been shown to be correlated at a scale of a few hundred kilometres by Fraedrich & Schönwiese (2002). When analysing boreholes in a cluster of small spatial extent, signals present only in a single borehole can be effectively suppressed (Beltrami *et al.* 1997).

In the algorithms commonly used for GSTH inversions, 1-D, purely conductive models are considered, as a homogeneous half-space (Beltrami *et al.* 1997) or a layered medium (e.g. Nielsen & Beck 1989; Shen & Beck 1991). Hartmann & Rath (2005) systematically investigated the effects of erroneous petrophysical parameters, and basal heat flow densities on the inversion results. It was shown that even moderately false assumptions may produce significant errors in the estimates. In the case studies presented here, thermal conductivity, diffusivity and heat production are well known as a function of depth from extensive petrophysical measurements (for the Kola borehole, see Mottaghy *et al.* 2005). Basal heat flow density has also been determined by independent methods (Mottaghy *et al.* 2005). In many cases, this information can be determined from a combination of temperature data with other geophysical logs, or obtained by some inverse techniques (e.g. Gallagher 1990; Gallagher & Sambridge 1992; Hartmann *et al.* 2005; Rath *et al.* 2006). The possibility of simultaneous inversion for palaeoclimate and physical properties is an active area of investigation.

When inverting borehole temperatures for GSTH using Tikhonov or related methods, a choice of the regularization parameter is necessary. This parameter controls the trade-off between the data fitting error and the model semi-norm applied for inversion. In particular, when comparing different data sets, methods, or results, it is important to give a repeatable and objective way of selecting its value. Common methods for choosing this parameter are, among others, the L-curve (Hansen 1992) or the Generalized Cross-Validation (GCV) criterion (Wahba 1990). Here, we concentrate on the latter method, while an example for the use of the former is given by Hartmann & Rath (2005).

This paper is organized as follows. First, the method employed is summarized in Section 2. After describing the forward model and the assumptions adopted in Section 2.1, the inversion algorithm is presented in Section 2.2. In particular, we describe the GCV method applied to find the optimum regularization parameter. This is followed by two case studies, one based on the Kola superdeep drilling site in Section 3, the other from a borehole in the sediments of Northeastern Poland in Section 4.

2 INVERSE METHOD

The solution of any inverse problem requires that the corresponding forward model is known and adapted to the physical processes involved. As the use of analytical solutions does not allow for appropriately complex situations, we use a straightforward numerical solution of the heat equation by finite difference methods. This gives us considerable freedom of introducing more realistic physics of the systems, as the non-linear dependencies of the system parameters on temperature and pressure, and, in particular, the effects of latent heat. However, as already pointed out above, we refrained from introducing fluid flow into the system.

2.1 Forward model

The 1-D, purely conductive heat equation in a porous medium can be written as:

$$\frac{\partial}{\partial z}\left(\lambda_e \frac{\partial T}{\partial z}\right) + h = (\rho c)_e \frac{\partial T}{\partial t}, \tag{1}$$

where λ is thermal conductivity ($\mathrm{W\,m^{-1}\,K^{-1}}$), ρ is density ($\mathrm{kg\,m^{-3}}$), c is the specific heat capacity ($\mathrm{J\,kg^{-1}\,K^{-1}}$), and h is volumetric heat production ($\mathrm{W\,m^{-3}}$). The subscript e marks effective parameters of the porous medium, and can be interpreted as properties of a two-phase mixture between solid rock and fluid-filled pore space. This mixture is characterized by porosity ϕ. Usually, the geometric mean is chosen for thermal conductivity, that is, $\lambda_e = \lambda_w^{\phi} \cdot \lambda_m^{(1-\phi)}$, with the indices w and m denoting the fluid and matrix contribution. Volumetric quantities like (ρc) are averaged arithmetically, taking $(\rho c)_e = \phi \rho_w c_w + (1-\phi)\rho_m c_m$.

For the palaeoclimate application we have in mind, eq. (1) usually is solved with the appropriate boundary conditions, namely a fixed but time-dependent temperature at the top ($z = z_0$),

$$T = T(t) \qquad \text{at} \qquad z = z_0, \tag{2}$$

and fixed heat flow at the bottom,

$$\frac{\partial T}{\partial z} = -\frac{q_b}{\lambda} \qquad \text{at} \qquad z = z_b. \tag{3}$$

eq. (1) is understood to allow all coefficients, boundaries and sources, to be non-linearly dependent on temperature. Most rocks matrix properties exhibit moderate dependencies on temperature, while pressure can safely be neglected for the depths under considered here (Chapman 1986). As we are aiming at deep boreholes constraining the history of ground surface temperature for some 10 000 yr, we have to extend the numerical model to depths of several 1000 m, and temperatures of up to 200 °C accordingly. This requires taking the temperature dependencies of the thermophysical properties into account. In many practical situations, the upper layers of the subsurface are of sedimentary origin and show considerable porosities up to 40 per cent. In this case the physical properties of the fluid have a distinct influence, as they change with temperature, but unlike the matrix, they are also pressure-sensitive. We implemented the relations given in Table 1, defining the temperature (and pressure in the case of fluid density) dependence of the physical parameters within the forward module. For the domain characteristic of the boreholes investigated in this study (>5000 m depth), we compared the fluid properties with the ones from Wagner & Pruß (2002), to make sure that deviations are in an admissible range (<2 per cent). Certainly, these errors are much smaller than the ones induced by neglecting of salinity which can play a major role in some permafrost environments (Ippisch 2001).

Eq. (1) is solved by a standard 1-D finite difference scheme, allowing for irregular grids, variable coefficients, time-dependent boundary conditions, and source terms. The resulting non-linearity is handled by a simple fixed-point iteration, which proved to be adequate to the problem. Time-stepping is done by a general two-level scheme, including the well-known Forward/Backward Euler and Crank–Nicholson schemes (see, e.g. Wood 1990) as special cases.

Table 1. Dependencies fluid and ice properties on temperature and pressure.

Property	Reference
$\lambda_f(T)$	Phillips *et al.* (1981)
$c_f(T)$	derived from enthalpy given by Zylkovskij *et al.* (1994), salinity neglected
$\rho_f(T, P)$	from Zylkovskij *et al.* (1994), salinity neglected
$\lambda_i(T)$, $c_i(T)$, $\rho_i(T)$	Lide (2000)

The simplified form of the heat equation used in the forward problem of palaeoclimate inversion is easily modified to incorporate the effects of the presence of the ice phase, which turned out to be of first-order importance for one of our case studies (see Section 4). Details of theory, implementation, and the validation of the approach can be found in Mottaghy & Rath (2006). The approach chosen is of course a simplification of a process, which is far more complicated than described here (Ippisch 2001). For the application to palaeoclimate inversion we have restricted ourselves to the simplified approach, as mainly processes with large time constants are important, and thus the processes in the upper few metres of the subsurface do not play a significant role for the reconstruction of palaeotemperatures at scales larger then a few years.

2.2 Inverse technique

Given observed data, that is, recent borehole temperature measurements as a function of depth, $d_i = T(z_i, t_0)$, the GSTH, $T(0, t)$, can be estimated by a regularized least-squares procedure. To achieve this, an objective function is set up to be minimized:

$$\Theta = \|\mathbf{W}_d[\mathbf{d} - \mathbf{g}(\mathbf{p})]\|_2^2 + \tau_0 \left\|\mathbf{W}_p^0(\mathbf{p} - \mathbf{p}_a)\right\|_2^2 + \tau_1 \left\|\mathbf{W}_p^1(\mathbf{p} - \mathbf{p}_a)\right\|_2^2, \tag{4}$$

Here, $\mathbf{d} - \mathbf{g}(\mathbf{p}) \equiv \mathbf{r}$ is the residual vector between the data $\mathbf{d}$ and the solution of the forward problem $\mathbf{g}(\mathbf{p})$ at these points for a given parameter vector $\mathbf{p}$. The weighted norm of this residual represents the data fit. Data weighting is introduced by $\mathbf{W}_d$, which is usually used to standardize the residuals, that is, its diagonal is set to the inverse square root of the data variance. The second term in eq. (4) is defined by the application of a linear operator $\mathbf{W}_p$ on the deviations of the model parameters $\mathbf{p}$ from their preferred values $\mathbf{p}_a$.

To solve the inverse problem we try to find the minimum of functional (4) by formally differentiating equating the result to zero. This leads to the well-known normal equation,

$$\begin{aligned}\left[(\mathbf{W}_d\mathbf{J})^T\mathbf{W}_d\mathbf{J} + \tau_0\left(\mathbf{W}_p^0\right)^T\mathbf{W}_p^0 + \tau_1\left(\mathbf{W}_p^1\right)^T\mathbf{W}_p^1\right]\delta\mathbf{p} \\ = (\mathbf{W}_d\mathbf{J})^T\mathbf{r} - \tau_0\left(\mathbf{W}_p^0\right)^T\mathbf{W}_p^0(\mathbf{p} - \mathbf{p}_a) - \tau_1\left(\mathbf{W}_p^1\right)^T\mathbf{W}_p^1(\mathbf{p} - \mathbf{p}_a),\end{aligned} \tag{5}$$

which can be iterated as a modified Gauss–Newton iteration with $\mathbf{p}^{k+1} = \mathbf{p}^k + \delta\mathbf{p}^k$, where $\boldsymbol{\delta}\mathbf{p}$ is determined for each iteration by eq. (5). The derivative matrix $\mathbf{J}$ (Jacobian) results from the differentiation of the residuals $\mathbf{d} - \mathbf{g}(\mathbf{p})$. It is defined as:

$$J_{ij} = \frac{\partial g_i}{\partial p_j},$$

where p_j are the model parameters. Differentiation is done by an adaptive method using divided differences.

To solve the linear system (5), an equivalent formulation can be found, which is very flexible and allows using a variant of the well-known conjugate gradient method for its solution:

$$\begin{bmatrix}\mathbf{W}_d\mathbf{J} \\ \tau_0^{\frac{1}{2}}\mathbf{W}^{\mathbf{0}}{}_p \\ \tau_1^{\frac{1}{2}}\mathbf{W}^{\mathbf{1}}{}_p\end{bmatrix}\delta\mathbf{p} = \begin{bmatrix}\mathbf{W}_d^T[\mathbf{d} - \mathbf{g}(\mathbf{p})] \\ -\tau_0^{\frac{1}{2}}\mathbf{W}_p^0(\mathbf{p} - \mathbf{p}_a) \\ -\tau_1^{\frac{1}{2}}\mathbf{W}_p^1(\mathbf{p} - \mathbf{p}_a)\end{bmatrix}. \tag{6}$$

This rectangular system of linear equations is efficiently solved in each iteration by conjugate-gradient type methods like CGLS or LSQR (Björck 1996; Hansen 1997). Methods using only the gradient of an objective function like the one defined in eq. (4), that is, the Jacobian only enters through the matrix-vector product $-\mathbf{J}^T\mathbf{r}$, may be a good alternative choice for the minimization technique. The most prominent of these are the variants of Nonlinear Conjugate Gradients (NLCG) or Quasi-Newton (QN) algorithms (see, e.g. Nocedal & Wright 1999). However, the above-mentioned methods make it difficult to optimize regularization parameters.

In the case of GSTH inversion, we parametrized the surface temperatures as a series of step functions for $\mathbf{p}$. Number and temporal spacing of steps are set *a priori*, leaving the temperature values for each period as inversion parameters. These parameters are associated to the time steps indirectly. The time discretization of the forward problem thus can be chosen following numerical requirements, independently from the inverse grid employed. Due to the diffusive character of the underlying physics, the use of a mesh spaced logarithmically in time and space is useful to reduce computing times.

2.3 Regularizing operators

In this study a smoothing operator will be used for regularization. We propose a combination of differential operators of different order, namely $\mathbf{L}_0 = \mathbf{I}$, and $\mathbf{L}_1$. This operator represents the discrete first derivative with respect to time, and is defined as

$$\mathbf{L}_1 = \Delta t^{-1}\begin{bmatrix}-1 & 1 & & & \emptyset \\ & -1 & 1 & & \\ & & \ddots & & \\ \emptyset & & & -1 & 1\end{bmatrix}. \tag{7}$$

The product of the matrix defined in eq. (7) with the parameter vector $\mathbf{p}$ may be interpreted as the discrete approximation of its first derivative by forward divided differences, where Δt is the time spacing of the inverse mesh, which is assumed to be constant for the moment.

If $\mathbf{L}_0$ is used, the minimum distance between the solution and the prior model is sought. This, however, often leads to solutions displaying unwanted short-period oscillations. Regularizing with the $\mathbf{L}_1$ operator penalizes solution roughness, and guarantee smooth solutions if the weighting parameter τ_1 is chosen large enough. The $\mathbf{L}_1$ operator as defined above favours 'flat' solutions (Hansen 1997).

In the GSTH inversions presented here, we used a temporal inversion grid which decreases logarithmically during the time of simulation. Also, we used only the difference matrix, neglecting the denominator in eq. (7). This amounts to weighting the derivative with a time dependent factor of $\overline{\Delta T} = 0.5(\Delta t^{n+1} + \Delta t^n)$. By this simple approach variations at late times are less damped than at early ones.

For the inversions shown below, we look for the best value of τ, where $\tau_0 = \text{const}$ and $\tau_1 = \tau\tilde{\tau}_1$ with the tilde denoting the fixed base value. In principle, however, also a two parameter search could be employed.

2.4 Choosing the optimum regularization parameter

Following Farquharson & Oldenburg (2004) we shortly describe the generalized cross-validation (GCV) method. Defining the appropriate value of the regularization parameter for the GCV criterion is based on the 'leave-out-one' lemma (Golub *et al.* 1979; Wahba 1990). There, the *linear* inverse problem considered, which

minimizes

$$\sum_{i=1}^{N}[d_i - g_i(\mathbf{p})]^2 + \tau\|\mathbf{p}\|_2^2, \tag{8}$$

with respect to the model $\mathbf{p}$, where $\mathbf{g}(\mathbf{p}) = \mathbf{Jp}$ is the forward model with matrix $\mathbf{J}$. The noise in every observation d_i is assumed to be Gaussian with a fixed standard deviation σ_0. If all but the kth observation are inverted, setting the regularization parameter to a trial value $\hat{\tau}$, the problem is now to find the model $\mathbf{p}^k$ which minimizes

$$\sum_{i=1, i\neq k}^{N}[d_i - g_i(\mathbf{p})]^2 + \hat{\tau}\|\mathbf{p}\|_2^2. \tag{9}$$

If $\hat{\tau}$ is a suitable value for the regularization parameter, the kth forward-modelled value $g_k[\mathbf{p}^k]$ is expected to be close to the omitted observation, d_k. Obviously, this procedure can be repeated for each observation i. If all the calculated values $g_k[\mathbf{p}^k]$ are close to their observed values d_k, the value of $\hat{\tau}$ can be considered appropriate for the regularization parameter. In Wahba (1990) an expression is derived, allowing to determine the GCV function without solving the inverse problem explicitly for each omitted observation.

The problem of inverting borehole temperatures for ground surface temperature histories is non-linear, and hence requires the use of an iterative procedure. It was shown in Haber & Oldenburg (2000) that the GCV criterion gives a good estimate of the regularization parameter, providing convergence of the non-linear inverse problem. Using the notations from Section 2.2 (eqs 4 and 5), the GCV function for the nth iteration is

$$GCV^n(\tau) = \frac{\left\|\mathbf{d} - \mathbf{g}\left(\mathbf{p}_\tau^n\right)\right\|_2^2}{\left\{\mathrm{trace}\left[\mathbf{I} - \mathbf{W}_d\mathbf{J}^{n-1}\mathbf{M}^{-1}(\mathbf{J}^{n-1})^T\mathbf{W}_d^T\right]\right\}^2}, \tag{10}$$

where

$$\mathbf{M} = (\mathbf{J}^{n-1})^T\mathbf{W}_d^T\mathbf{W}_d\mathbf{J}^{n-1} + \tau_0\left(\mathbf{W}_p^0\right)^T\mathbf{W}_p^0 + \tau_1\left(\mathbf{W}_p^0\right)^T\mathbf{W}_p^0, \tag{11}$$

and τ_{GCV} is found by the minimum of eq. (10). In the inverse problem discussed in this work, when starting the iterations, an interval for this parameter is chosen, which is gradually narrowed during the following iterations. This reduces the number of calculations necessary for the GCV function. The effort can be further reduced by combining this method with a cooling-type procedure, where an initial (sufficiently large) value of τ is constantly reduced for a few iterates before GCV is invoked.

In order to demonstrate the power of the proposed method, we give a synthetic example. For this simulation, we used a single step at 15 ka before present (BP), rising from -10 to 5 °C as forcing function. Subsequently this step was smoothed with a 5-point triangular smoothing filter to reduce numerical problems caused by this discontinuity. The resulting synthetic borehole log was then perturbed adding Gaussian noise $\mathcal{N}(0, \sigma_n)$, assuming a standard deviation $\sigma_n = 0.25$ K for the numerical experiment shown below.

Physical parameters for this the simulation were as following. Neglecting heat production, we assumed a rock thermal conductivity of 3 W m^{-1} K^{-1}, a homogeneous porosity ϕ of 0.3, and a value of 1.9 MJ m^{-3} > for $(\rho c)_m$. The model extended to a depth of 3 km (500 cells) to prevent boundary effects in the numerical solution for the long simulation time 150 ka (500 time steps). At the base of the model a heat flux density of 35 mW m^{-2} was imposed.

In Fig. 1(a), the synthetic temperature profile is plotted, while Fig. 1(b) shows the inverted GSTH. It also demonstrates the influence of the regularization parameters on the reconstructed GSTH in the *last iteration*: the red line is the model determined by using the regularization parameter found at the minimum of the GCV function. However, the other models are plotted in different grey scales, the darker the closer to the minimum. The resulting GSTH reproduces quite well the form of the true model, though there are still some artefacts like the maximum near 3 ky. We believe this is due to the known fact that using GCV estimates for the regularization parameter can cause to much structure in the model (Walker 1999; Krakauer *et al.* 2004).

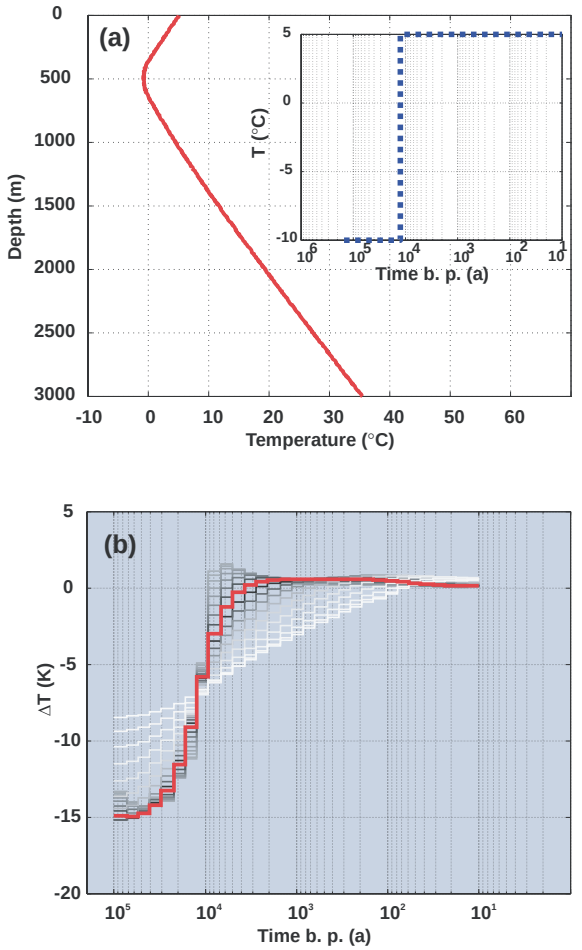

Figure 1. Results from a GSTH reconstruction from a synthetic example with an optimized regularization parameter. (a) Synthetic temperature log resulting from the forcing function in the inset. The forcing function is a single step at 15 ka BP with an amplitude of 15 K. (b) Reconstructed GSTH for the last iteration (red). Also shown are results for different values of the regularization parameters at this iteration, where the grey scale indicates the distance to the minimum. Darker curves correspond to values closer to the minimum.

Fig. 2(a) shows the resulting GSTH, where the iteration process is made visible by different colours. The models for every iteration are obtained with an optimized regularization parameter τ, found by the minimum of the GCV function, which is plotted in Fig. 2(b) versus τ. Here, the iteration number is given by the colour-code.

Though the GCV method was used in a straightforward manner in this study, we mention that optimum values of the regularization parameters can also be found by more advanced techniques, if computer resources become important due to the size of the problem (see Golub & von Matt 1996). An alternative method to speed up the solution of eq. (6) for multiple τ is a modification of CGLS

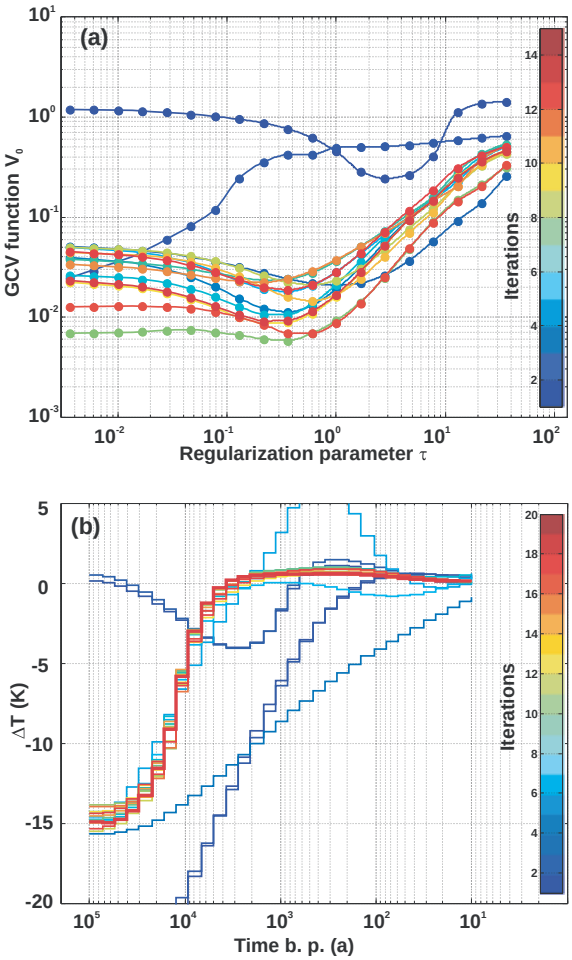

Figure 2. Behaviour of GCV function for the synthetic example shown in Fig. 1. (a) Reconstructed GSTH for the all 15 iterations. (b) GCV functions for each iteration, also colour coded. The first few non-linear iterations are still far away from the optimum. This also shows up in the behaviour of the GCV function, which converge to a stable value only in the later iterations. The first five iterations were run with fixed $\tau_0 = 3$ and $\tau_1 = 50$.

algorithm suggested by Frommer & Maass (1999) and van den Eshof & Sleijpen (2004).

3 CASE STUDY 1: KOLA PENINSULA, RUSSIA

For this case study we analysed data from the Russian ultradeep borehole on the Kola Peninsula (SG-3, Fig. 3). The full temperature data set was published by Popov *et al.* (1999) and shown in Fig. 4(a). For the present study, the top 500 m, and the parts below 3500 m had to be neglected due to obvious effects of fluid flow or other still unknown features (Mottaghy *et al.* 2005). Therefore, we used only a part of this temperature log. With respect to thermal properties, we used the extensive measurements on core samples from SG-3, performed by Popov *et al.* (1999). This gave us the opportunity to set up a detailed model of the thermal properties of the subsurface. Temperature data were available at an interval of 20 m, while thermal conductivity was available at intervals between 30 and 50 m. As our forward model was discretized on a log-spaced vertical grid, we had to smooth the data and subsequently interpolate them to the grid cells. Additionally, temperature dependencies for the different rock

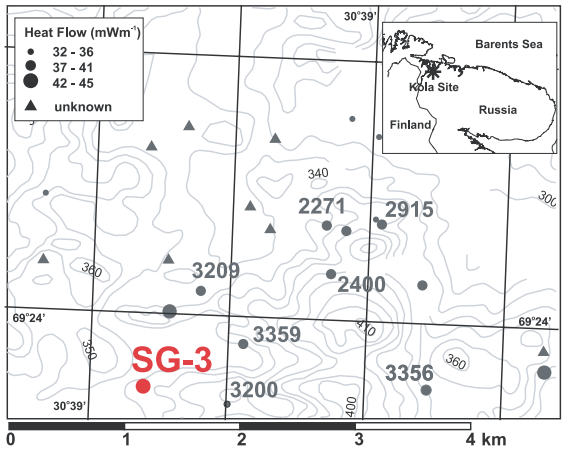

Figure 3. Location of the Kola superdeep borehole (red symbol). Grey symbols mark the boreholes used for the determination of the temperature dependencies as mentioned in the text.

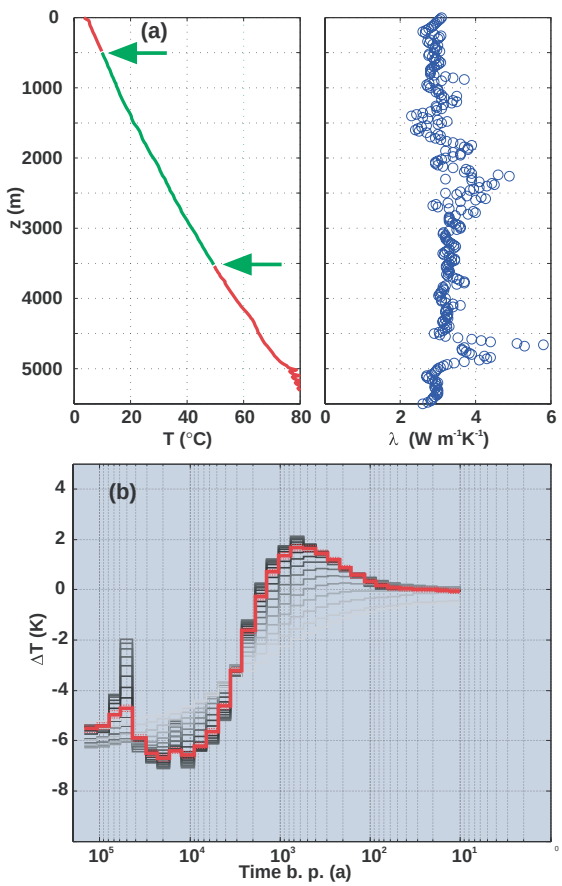

Figure 4. Results from GSTH reconstruction for the Kola superdeep borehole with an optimum regularization parameter. Panel (a) shows the temperature log and the thermal conductivity distribution. The arrows mark the interval used for the GSTH inversion. (b) Reconstructed GSTH for the last iteration (red) (see also Fig. 1).

types were determined on a larger number of samples collected in shallower boreholes in the surrounding of the superdeep borehole (Mottaghy *et al.* 2005). The resulting relations for the temperature dependencies of λ_m and $(\rho c)_m$ were implemented in the forward modelling code.

In the case of SG-3 the numerical model extended to a depth of 6000 m, discretized by 300 log-spaced cells. We started the simulation at 150 ka BP, while time integration was achieved with logarithmically decreasing step using Crank–Nicholson weighting (Strikwerda 2004).

The best fit to the borehole data was obtained with a recent mean annual ground surface temperature of 3.5 °C, which is consistent with the studies of Popov *et al.* (1999). For this study, we could rely on a large number of well-determined thermal properties. This lead us to assume that the basal heat flow determined from the temperatures is well constrained to approximately, 48 mW m^{-2} at a depth of 6000 m, where the effect of heat production is taken into account.

We applied the GCV procedure described in Section 2.4 to this data set, using a zero prior model. The results are shown in Fig. 4(b). In this case the GCV functions are rather flat for small values of τ in the last iterations (Fig. 5a). It is still possible to identify a stable minimum, though it is quite wide. The corresponding curves between $\tau = 1$ and 10 yield practically the same GSTH. Nevertheless, Fig. 5(b) shows that both lower and higher values of τ yield significantly rougher or smoother models, respectively.

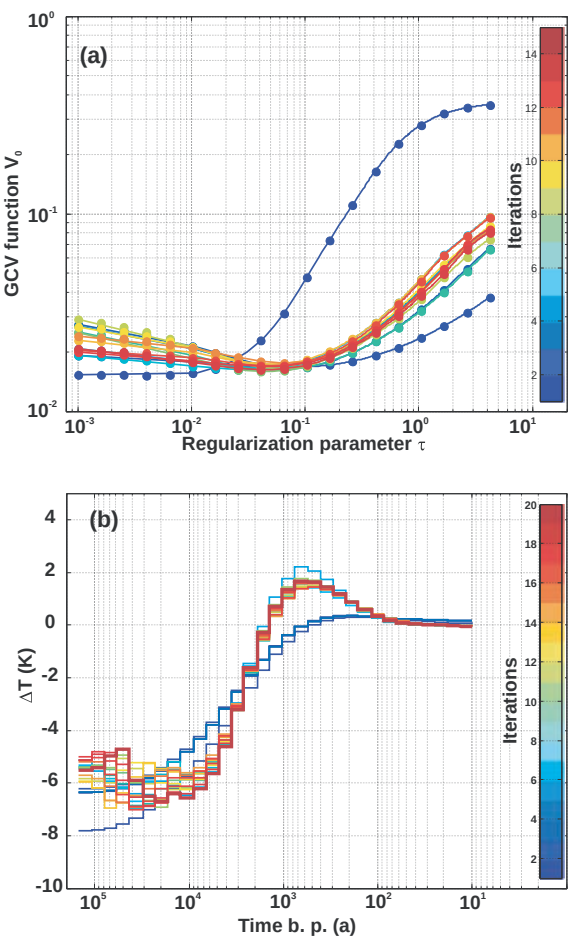

Figure 5. Behaviour of the GCV function for the Kola superdeep borehole. (a) Reconstructed GSTH for the all 15 iterations. (b) GCV functions for each iteration, also colour coded. In contrast synthetic model, a stable solution, and a consistent behaviour of the GCV function are found already in the very early iterations. The first five iterations were run with fixed $\tau_0 = 0.7$ and $\tau_1 = 50$.

Figure 6. Location of the UDRYN borehole (red symbol).

4 CASE STUDY 2: UDRYN, NORTHEASTERN POLAND

A second field example uses data from the UDRYN IG-8 borehole (see Fig. 6), which were already presented in Šafanda *et al.* (2004) and Mottaghy & Rath (2006). In this borehole not only temperature data were available, but also porosities and thermal conductivities reconstructed from borehole wireline logging. We used a simple layered model compiled by Majorowicz (2005, personal communication). The data for this borehole is shown in Fig. 7(a).

In contrary to SG-3, knowing the porosity is important, as porosities are high enough to expect a significant impact of the thawing/freezing process. For the inversion we had to set the extent of the forward model to a depth of 6000 m, assuming the properties below the depth of the borehole to be mean bedrock properties as found in the borehole below 900 m. For the temperature dependence of the thermal properties of the rocks, we adopted the formulations given by Haenel *et al.* (1988) for thermal conductivity, and Herrmann (1999) for heat capacity. Water and ice properties were calculated as a function temperature and pressure (see Table 1).

For this inversion we used the same temporal and spatial setup as in the case of SG-3. The best fit to the borehole data was obtained with a recent mean annual temperature of 7 °C, which is slightly above the mean annual air temperature (2 m height) at the location of the borehole (≈6 °C). As we took the thermal conductivity to be basically correct, there is not much freedom to vary the basal heat flow, which was set to 38.4 mW m^{-2} at a depth of 6000 m, accounting for heat production. This corresponds to a surface heat flow of 41.4 m^{-2}, which has been determined by Majorowicz (2005, personal communication). Again, the temperature data were smoothed and interpolated to the grid used for the modelling. We assumed a logarithmic temporal grid, starting with large time steps in the past from 150 ky to small steps up to the present.

For the inversion, this time a non-zero prior is used. We chose a step function rising from −8 to 0 °C at 15 ka BP, which was smoothed to avoid artefact resulting from discontinuous priors. This choice was inspired by the mean GSTH for Fennoscandia and the East European Platform given by Kukkonen & Joeleht (2003). As their data base includes areas of varying times of ice coverage, this may be considered as a conservative estimate.

Fig. 7(b) shows the resulting GSTH. From Figs 8(a) and (b) it becomes evident that the GCV function stabilizes only after several iterations. In this case the chosen strategy of running the first few iterations with a fixed, sufficiently large regularization parameter

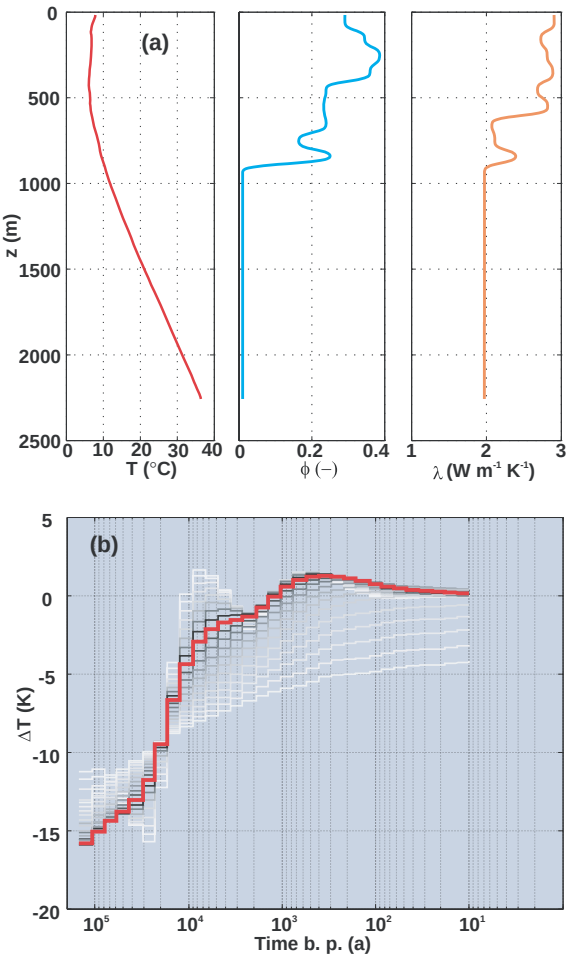

Figure 7. Application of the GCV technique to the UDRYN borehole (Northeastern Poland). (a) Temperature log, porosity, and the thermal conductivity distribution. (b) Reconstructed GSTH for the last iteration (red) (see also Fig. 1).

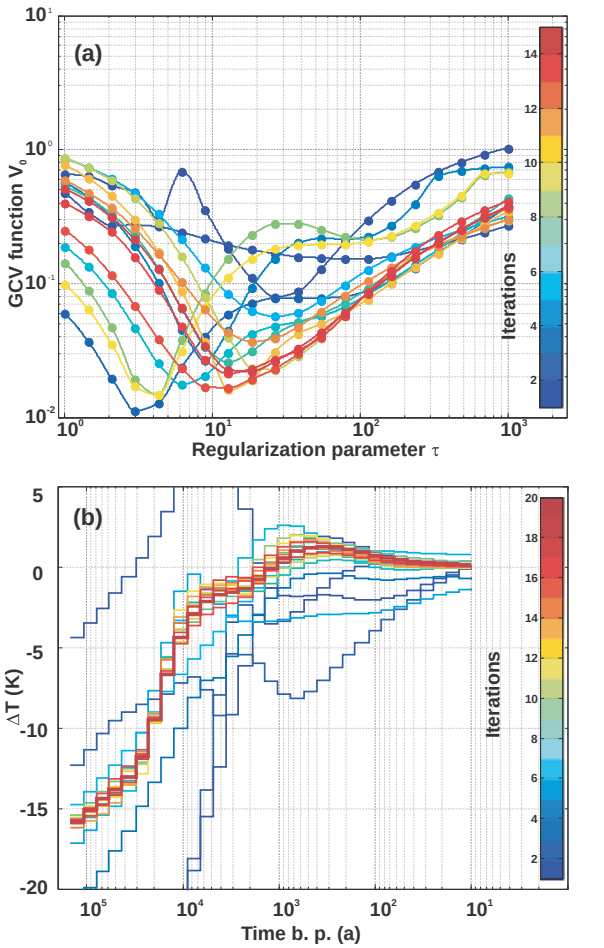

Figure 8. Behaviour of the GCV function for the UDRYN borehole. (a) Reconstructed GSTH for the all 15 iterations. (b) GCV functions for each iteration, also colour coded. The first few non-linear iterations are still far away from the optimum. As for the synthetic model, the GCV functions converge to a stable value only in the later iterations, where the GCV criterion is used for the model update. The first five iterations were run with fixed $\tau_0 = 1$ and $\tau_1 = 10$.

was crucial. Additionally, without the assumed prior, convergence was difficult to achieve.

5 DISCUSSION

The specific method applied in this study raises several questions.

First of all, one may argue that the rather fine temporal discretization used may be an overparametrization. It is indeed, given the resolution of borehole temperatures. However, it is one possibility for combining flexibility with respect to the unknown time history of GST with the easy incorporation of prior knowledge. Due to the fine resolution of the step function used for driving the model, the assumptions about the palaeotemperature history are kept to a minimum. Furthermore, a setup of steps which is equidistant on a logarithmic scale leads to a well-adapted inverse mesh, placing more parameters where resolution is possibly high, and less where only long-period signals have survived.

The necessity for regularization is obvious in a severely ill-posed problem like GSTH inversion. The approach taken in this study uses a combination of Tikhonov regularization operators, which at first glance may be thought to be arbitrary. However, our particular choice for the regularization matrix can be understood in an informal way from a Bayesian point of view. There is a close connection of difference operators to the inverse covariances used in this approach. It has been pointed out (Tarantola 1987; Yanovskaya & Ditmar 1990; Tarantola 2004; Xu 2005) that the inverses of common covariance matrices (for instance, the Markovian or Gaussian) may be approximated by a series built from differential operators. The regularization chosen is thus a simple way to enforce temporal correlation to the solution of the inverse problem. Additionally, in our scheme usually a logarithmic inversion grid is employed. This takes into account the decreasing resolution of borehole temperatures with depth, at the price of additional error when approximating the derivatives.

Both field data sets were cleaned for near-surface or other spurious effects. As already mentioned above, Kola SG-3 was used from 500 to 3500 m, leaving the last millennium badly constrained by the data, but strongly influenced by the prior model and regularization. In this case, a zero prior GSTH was used. This explains the smooth behaviour of the latter for the last few hundreds of years, where no data were available.

At the UDRYN site, the situation is similar, with the top of the data used at 150 m. This implies that the apparent medieval climatic optimum in both of these places may be an artefact of the

smoothing technique and the missing data for the top few hundreds of meters. GST changes before 2 ka BP will probably not be resolved by the data, but will reflect the chosen prior. This due both to the low resolution of the method at large depths, the uncertainties in the model such as the heat flow estimate used, and the limited data.

The case studies, however, have shown that the total amount of warming after the glacial maximum is well constrained by both data sets. The Kola SG-3 study with the rather small warming step of 7 K is consistent with the values obtained by Kukkonen & Joeleht (2003) by MC inversion for Fennoscandia, who give an average of 8 $\pm$ 4.5 K (10 ka BP). Combined with the recent surface temperature of $\approx$3.5 $^\circ$C, this implies a minimum value of $-$3.5 $^\circ$C. At UDRYN, however, the total warming has been much larger, amounting to nearly 15 K. This is again consistent with other deep European sites, for example, the KTB pilot site (southeastern Germany) with a warming of about 10 K (Clauser & Mareschal 1995). Kukkonen & Joeleht (2003) have already pointed out that large parts of the Weichselian ice sheet were at temperatures of a few K below zero even at the glacial maximum (probably more than 50 per cent, see Boulton *et al*. 2001; Forsström 2005). Present-day GSTH inversion can only recover this basal temperatures, which are considerably higher than air temperatures. In contrary to the northern Kola Peninsula, the UDRYN area has been covered by ice only for a very short time, being exposed to cold air conditions most of the Weichselian period. The missing long-term glaciation at this site may explain the difference in estimated temperatures since in the late Pleistocene.

6 CONCLUSIONS

We have presented a method for choosing the optimum regularization parameter in smooth palaeoclimate inversions. From our experience we conclude that this a promising technique for making the GSTH inversions more automatic and more objective. Manual intervention of the interpreter is reduced in the sense that once model and regularizing operator are selected, the trade-off parameter is chosen in a repeatable manner.

We have demonstrated the power of this approach both on synthetic data. Though the convergence histories display quite different features in the three cases, a satisfactory final result was obtained in each of them. Nonetheless, more experience with different data constellations are necessary, and a comparison with other techniques is advisable, in particular, the L-curve criterion (Hansen 1992; Farquharson & Oldenburg 2004). Much more important, however, are further investigations into better-adapted regularizing operators, which may imply more, and in particular better prior information on GSTH behaviour. One possible candidate for this could be the minimum (gradient) support method (see Portniaguine & Zhdanov 1999; Zhdanov 2002), or wavelet methods.

Though far from being final, the results from the two case studies presented here have shown that the presence of a glacial ice shield has important consequences for the interpretation of many high-latitude GSTH inversion data. Its base being at rather high temperatures in most areas, GSTH inversions will only recover this temperatures, depending on the length of the glaciation period.

ACKNOWLEDGMENTS

Thanks to Y. Popov, J. Majorowicz and J. Safanda, who made available the field data used in the case studies presented here. Thoughtful reviews by K. Gallagher, N. Balling and B. H. Jacobsen improved this study considerably.

REFERENCES

Beltrami, H., Cheng, L. & Mareschal, J.C., 1997. Simultaneous inversion of borehole temperature data for determination of ground surface temperature history, *Geophys. J. Int.*, **129,** 311–318.

Björck, Å., 1996. *Numerical Methods for Least Squares Problems*, SIAM, Philadelphia.

Boulton, G.S., Dongelmans, P., Punkari, M. & Broadgate, M., 2001. Paleoglaciology of an ice sheet through a glacial cycle: the European ice sheet through the Weichselian, *Quater. Sci. Revi.*, **20,** 591–625.

Chapman, D.S., 1986. Thermal gradients in the continental crust, in *The Nature of The Lower Continental Crust*, eds Dawson, J.B., Carswell, D.A., Hall, J. & Wedepohl, K.H., Geological Society Special Publication No. 24, Blackwell Scientific Publications, Oxford.

Clauser, C. & Mareschal, J.C., 1995. Ground temperature history in central Europe from borehole temperature data, *Geophys. J. Int.*, **121**(3), 805–817.

Dahl-Jensen, D., Mosegaard, K., Gundestrup, N., Clow, G.D., Johnsen, S.J., Hansen, A.W. & Balling, N., 1998. Past temperatures directly from the greenland ice sheet, *Science*, **282,** 268–271.

Farquharson, C.G. & Oldenburg, D.W., 2004. A comparison of automatic techniques for estimating the regularization parameter in non-linear inverse problems, *Geophys. J. Int.*, **156,** 411–425.

Ferguson, G., Beltrami, H. & Woodbury, A.D., 2006. Perturbation of ground surface temperature reconstructions by groundwater flow? *Geophys. Res. Lett.*, **33,** L13708.

Forsström, P.-J., 2005. Through a glacial cycle: simulation of the Eurasian ice sheet dynamics during the last glaciation, *Ann. Acad. Sci. Fennicae Geologica-Geographica*, **168,** 1–94.

Fraedrich, K. & Schönwiese, C.-D., 2002. Space-time variability of the European climate, in *The Science of Desaster: Climate Disruptions, Heart Attacks, and Market Crashes*, pp. 120–155, eds Bunde, A., Kropp, J. & Schellnhuber, H., Springer Verlag, Berlin.

Frommer, A. & Maass, P., 1999. Fast CG-based methods for Tikhonov-Phillips regularization, *SIAM J. Sci. Comp.*, **20**(5), 1831–1850.

Gallagher, K., 1990. Some strategies for estimating present day heat flow from exploration wells, *Explor. Geophys.*, **21,** 145–159.

Gallagher, K. & Sambridge, M., 1992. The resolution of past heat flow in sedimentary basins from non-linear inversion of geochemical data: the smoothest model approach, with synthetic examples, *Geophys. J. Int.*, **109,** 78–95.

Golub, G.H. & von Matt, U., 1996. Generalized cross-validation for large scale problems, Tech. Rep. TR-96-28, Swiss Center for Scientific Computing, ETH Zürich, CSCS/SCSC.

Golub, G.H., Heath, M. & Wahba, G., 1979. Generalized cross-validation as a method for choosing a good ridge parameter, *Technometrics*, **21,** 215–223.

Haber, E. & Oldenburg, D., 2000. A GCV based method for nonlinear ill-posed problems, *Comput. Geosci.*, **4**(1), 41–63.

Haenel, R., Rybach, L. & Stegena, L., 1988. *Handbook of Terrestrial Heat-Flow Density Determination*, Kluwer, Dordrecht, Holland.

Hansen, P.C., 1992. Analysis of ill-posed problems by means of the L-curve, *SIAM Rev.*, **34,** 561–580.

Hansen, P.C., 1997. *Rank Deficient and Discrete Ill-Posed Problems. Numerical Aspects of Linear Inversion*, SIAM, Philadelphia.

Hartmann, A. & Rath, V., 2005. Uncertainties and shortcomings of ground surface temperature histories derived from inversion of temperature logs, *J. Geophys. Eng.*, **2,** 299–311.

Hartmann, A., Rath, V. & Clauser, C., 2005. Thermal conductivity from core and well log data, *Int. J. Rock Mech. Min. Sci.*, **42,** 1042–1055.

Herrmann, H., 1999. Numerische Simulation reaktiver Strömungen im porösen Untergrund am Beispiel der Lösung und Ausfällung, *PhD thesis*,

Mathem.-Naturw. Fakultät, Rheinische Friedrich-Wilhelms-Universität Bonn.

Huang, S., Pollack, H.N. & Shen, P.-Y., 2000. Temperature trends over the past five centuries reconstructed from borehole temperatures, *Nature*, **403,** 756–758.

Ippisch, O., 2001. Coupled Transport in Natural Porous Media, *PhD thesis*, University of Heidelberg.

Kohl, T., 1998. Palaeoclimatic temperature signals—can they be washed out? *Tectonophysics*, **291,** 225–234.

Krakauer, N.Y., Schneider, T., Randerson, J.T. & Olsen, S.C., 2004. Using generalized cross-validation to select parameters in inversions for regional carbon fluxes, *Geophys. Res. Lett.*, **31,** L19108.

Kukkonen, I.T. & Joeleht, A., 2003. Weichselian temperatures from geothermal heat flow data, *J. geophys. Res.*, **108**(B3), 2163, doi:10.1029/2001JB001579.

Lide, D., ed., 2000. *Handbook of Chemistry and Physics*, 81st edn, CRC Press, Boca Raton, FL, USA.

Mottaghy, D. & Rath, V., 2006. Latent heat effects in subsurface heat transport modeling and their impact on paleotemperature reconstructions, *Geophys. J. Int.*, **164**(1), 236–245.

Mottaghy, D., Popov, Y.A., Schellschmidt, R., Clauser, C., Kukkonen, I.T., Nover, G., Milanovsky, S. & Romushkevich, R.A., 2005. New heat flow data from the immediate vicinity of the Kola superdeep borehole: vertical variation in heat flow density confirmed, *Tectonophysics*, **401**(1–2), 119–142.

Nielsen, S.B. & Beck, A.E., 1989. Heat flow density values and paleoclimate determined from stochastic inversion of four temperature-depth profiles from the Superior Province of the Canadian Shield, *Tectonophysics*, **164,** 345–359.

Nocedal, J. & Wright, S.J., 1999. *Numerical Optimization*, Springer, New York.

Phillips, S.L., Igbene, A., Fair, J.A., Ozbek, H. & Tavana, M., 1981. A technical data book for geothermal energy utilization, Tech. Rep. 12810, Lawrence Berkeley Labartory.

Pollack, H.N., Huang, S. & Shen, P., 1998. Climate change record in subsurface temperatures: a global perspective, *Science*, **282,** 279–281.

Popov, Y.A., Pevzner, S.L., Pimenov, V.P. & Romushkevich, R.A., 1999. New geothermal data from the Kola superdeep well SG-3, *Tectonophysics*, **306,** 345–366.

Portniaguine, O. & Zhdanov, M.S., 1999. Focusing geophysical inversion images, *Geophysics*, **64,** 874–887.

Rath, V., Wolf, A. & Bücker, M., 2006. Joint three-dimensional inversion of coupled groundwater flow and heat transfer based on automatic differentiation: sensitivity calculation, verification, and synthetic examples, *Geophys. J. Int.*, **167,** 453–466.

Šafanda, J. & Rajver, D., 2001. Signature of the last ice age in the present subsurface temperatures in the Czech Republic and Slovenia, *Global Planet. Change*, **29,** 241–257.

Šafanda, J., Szewzyk, J. & Majorowicz, J.A., 2004. Geothermal evidence of very low glacial temperatures on a rim of the Fennoscandian ice sheet, *Geophys. Res. Lett.*, **31,** L07211.

Shen, P.Y. & Beck, A.E., 1991. Least squares inversion of borehole temperature measurements in functional space, *J. geophys. Res.*, **96**(B12), 19 965–19 979.

Strikwerda, J.C., 2004. *Finite Difference Schemes and Partial Differential Equations*, 2nd edn, SIAM, Philadelphia, PA.

Taniguchi, M., 1993. Evaluation of vertical groundwater fluxes and thermal properties of aquifers based on transient temperature-depth profiles, *Water Resour. Res.*, **29**(6), 2021–2026.

Tarantola, A., 1987. *Inverse problem theory. Methods for data fitting and model parameter estimation*, Elsevier, Amsterdam.

Tarantola, A., 2004. *Inverse Problem Theory. Methods for Model Parameter Estimation*, SIAM, Philadelpha, http://www.ipgp.jussieu.fr/tarantola/Files/Professional/Books/index.html.

van den Eshof, J. & Sleijpen, G.S.L., 2004. Accurate conjugate gradient methods for shifted systems, *Appl. Numer. Math.*, **49**(1), 17–37.

Vasseur, G., Demongodin, L. & Bonneville, A., 1993. Thermal modelling of fluid flow effects in thin-dipping aquifers, *Geophys. J. Int.*, **112,** 276–289.

Wagner, W. & Pruß, A., 2002. The IAPWS formulation 1995 for the thermodynamic properties of ordinary water substance for general and scientific use, *J. Phys. Chem. Ref. Data*, **31,** 387–535.

Wahba, G., 1990. *Spline Models for Observational Data*, SIAM, Philadelphia.

Walker, S.E., 1999. Inversion of EM data to recover 1-D conductivity and a geometric survey parameter, *Master's thesis*, University of British Columbia.

Wood, W.L., 1990. *Practical Time-Stepping Schemes*, Clarendon, Oxford.

Xu, Q., 2005. Representations of inverse covariances by differential operators, *Adv. Atmos. Sci.*, **22**(2), 181–198.

Yanovskaya, T.B. & Ditmar, P.G., 1990. Smoothness criteria in surface wave tomography, *Geophys. J. Int.*, **102,** 63–72.

Zhdanov, M.S., 2002. *Geophysical Inverse Theory and Regularization Problems*, Elsevier, Amsterdam.

Zschocke, A., Rath, V., Grissemann, C. & Clauser, C., 2005. Quantifying deep fluid flow in inclined reservoirs from correlated discontinuities in vertical heat flow, *J. Geophys. Eng.*, **2,** 332–342.

Zylkovskij, G.A., Robinson, B.A., Dash, V.B. & Trease, L.L., 1994. Models and methods summary for the FEHMN application, Tech. Rep. LA-UR-94-3787, Los Alamos Natioal Laboratory.